

## How does a periodic rotating wave emerge from high-dimensional chaos in a ring of coupled chaotic oscillators?

 Ying Zhang,<sup>1,\*</sup> Gang Hu,<sup>2</sup> and Hilda A. Cerdeira<sup>1</sup>
<sup>1</sup>The Abdus Salam International Centre for Theoretical Physics, P. O. Box 586, 34100 Trieste, Italy

<sup>2</sup>Department of Physics, Beijing Normal University, Beijing 100875, China

(Received 16 February 2001; revised manuscript received 17 May 2001; published 21 August 2001)

A route to typical rotating waves from high-dimensional chaos is investigated in diffusively coupled chaotic Rössler oscillators. By increasing the coupling from zero, a high-dimensional spatiotemporal chaos changes into a coherent state, which is periodic in time and well ordered in space, through consecutive transitions. A crossover transition from spatially random chaos to spatially ordered chaos with phase locking and orientational equality (for two directions) breaking is a crucial step for establishing the typical spatial order of the rotating wave.

DOI: 10.1103/PhysRevE.64.037203

PACS number(s): 05.45.Xt, 05.45.Jn

The dynamics of networks of coupled oscillators is a fundamental problem. In many applications, the oscillators are identical, dissipative, and the coupling is symmetric. Since Turing's seminal work [1] on morphogenesis, rings of coupled oscillators have been used extensively in physiological and biochemical studies [2,3], coupled laser systems, Josephson junction arrays, electrical circuits, coupled chemical oscillators, etc. [4–6]. In early studies, interest focused on coupled periodic oscillators [3]. During the recent decade, interest has turned to the study of coupled chaotic oscillators. Rich behavior of chaotic and regular patterns associated with various kinds of chaos synchronization has been revealed [7]. With weak coupling the ring of the oscillators shows high-dimensional spatiotemporal chaos. With certain intermediate coupling we can, usually, observe some regular patterns with both spatial and temporal orders. For instance, rotating waves are typical patterns with these orders. It is important to understand how spatiotemporal chaos can be changed to a rotating wave state by continually varying a certain control parameter, in particular, how the spatial order of the rotating wave is established in this variation process. To our knowledge, this problem has not been clearly answered, and this is the central focus of the present paper. We shall show that the spatial order of the antiphase distribution of oscillators is established far before the rotating wave appears. An average-antiphase distribution can occur in a high-dimensional chaotic state via phase synchronization of chaos. This synchronization is the root of the spatial order of the periodic rotating wave.

We take the coupled Rössler oscillators as our model:

$$\begin{aligned} \dot{x}_i &= -y_i - z_i + \varepsilon(x_{i+1} + x_{i-1} - 2x_i), \\ \dot{y}_i &= x_i + ay_i + \varepsilon(y_{i+1} + y_{i-1} - 2y_i), \\ \dot{z}_i &= b + (x_i - c)z_i + \varepsilon(z_{i+1} + z_{i-1} - 2z_i), \end{aligned} \quad (1)$$

$$x_{i+n} = x_i, \quad y_{i+n} = y_i, \quad z_{i+n} = z_i, \quad i = 1, 2, \dots, n.$$

For  $a=0.45$ ,  $b=2.0$ , and  $c=4.0$ , the single Rössler oscillator is chaotic. In most of the paper, we fix the system size to  $n=6$ , and an extension to general system size will be briefly discussed later in this work. For small coupling,  $\varepsilon \ll 1$ , the motion is high-dimensional chaos, and it is chaotic in time and disordered in space [see Fig. 1(a)]. However, for certain intermediate coupling, the motion becomes regular. For instance, a stable rotating wave solution exists in the range of  $0.057 < \varepsilon < 0.090$  [8]. In Fig. 1(b), we fix  $\varepsilon=0.080$ , where we can see a rotating wave solution, which has a typical  $Z_6$  spatial symmetry [9], and it is periodic in time and well ordered in space. In this state, all oscillators take an identical periodic orbit, but they have equal phase shift  $T/6$  between each pair of nearest-neighbor oscillators with  $T$  being the period of the motion. In this paper we call this kind of phase distribution the antiphase distribution [6].

To answer the problem of how the disordered and chaotic state of Fig. 1(a) can develop into the regular state of Fig. 1(b) with both temporal and spatial orders, we first briefly report on the observations of numerical results by increasing the coupling strength from zero with a coarse step  $\Delta\varepsilon=0.001$ . We find there are several major steps in this variation. First, the spatially disordered chaos [ $C_D$ ] shown in Fig. 1(a) transit to a chaotic state with average-antiphase distri-

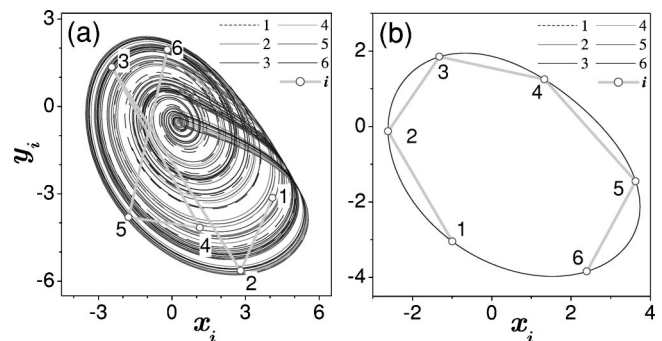


FIG. 1. The orbits of Eqs. (1) in  $(x, y)$  space. (a)  $\varepsilon=0.005$  (the disordered chaos state). (b)  $\varepsilon=0.080$  (the rotating wave). The numbers  $i=1, 2, \dots, 6$  in the figures indicate the positions of the  $i$  oscillator at an arbitrary instant. The notation same is also used in Fig. 2.

\*Email address: yzhang@ictp.trieste.it

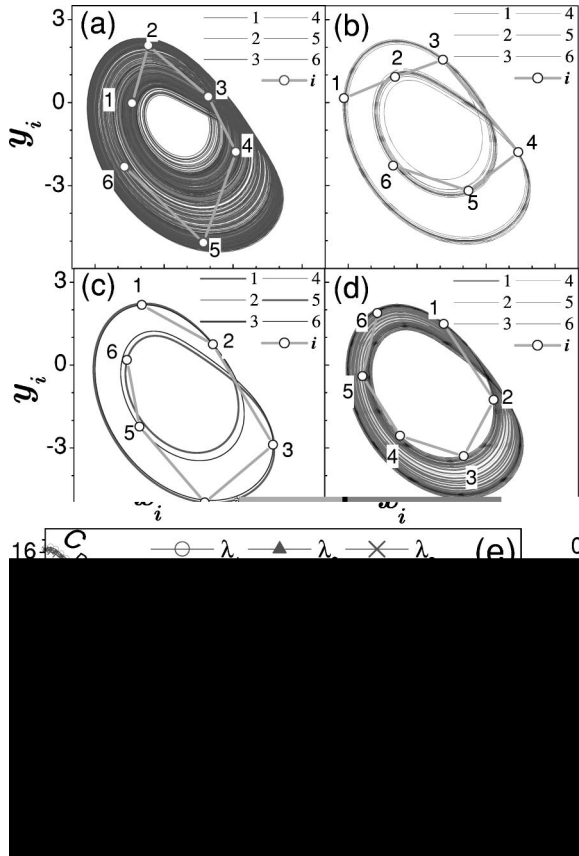


FIG. 2. (a) Orbit of  $C_A$  with  $\varepsilon=0.018$ . (b) Orbit of  $P_6$  with  $\varepsilon=0.024$ . (c) Orbit of  $P_2$  with  $\varepsilon=0.030$ . (d) Orbit of  $Q_1$  with  $\varepsilon=0.045$ . (e) Three largest Lyapunov exponents vs  $\varepsilon$  from zero to 0.090 with a coarse step as  $\Delta\varepsilon=0.001$ .

bution [ $C_A$ ] shown in Fig. 2(a). By “average-antiphase” we mean that the phase angles of the oscillators  $\phi_i$  [ $\tan \phi_i(t) = y_i(t)/x_i(t)$ ] have a well-ordered equal-phase separation in long-time average

$$\langle \Delta_{i+1,i} \rangle = \lim_{T \rightarrow \infty} \frac{1}{T} \int_0^T [\phi_{i+1}(t) - \phi_i(t)] dt = 2\pi/n, \quad i=1,2,\dots,n. \quad (2)$$

Second, the chaotic average-antiphase state develops to a periodic average-antiphase state shown in Fig. 2(b), in which the six oscillators perform periodic motions different from each other, which is then called  $P_6$ . Third, this periodic state with six distinctive attractors, can be replaced by another kind of periodic average-antiphase state by further increasing  $\varepsilon$  shown in Fig. 2(c), which satisfies  $Z_3$  symmetry [9]. The six oscillators occupy two kinds of attractors  $A$  and  $B$ , called  $P_2$ , and in the order from 1 to 6 they take trajectories as  $A$ ,  $B$ ,  $A(t+T/3)$ ,  $B(t+T/3)$ ,  $A(t+2T/3)$ , and  $B(t+2T/3)$ . Fourth, a quasiperiodic average-antiphase state, in which all oscillators share an identical attractor, called  $Q_1$ , appears [see Fig. 2(d)] in the range of  $0.034 < \varepsilon < 0.057$ , after which the periodic rotating wave of Fig. 1(b), called  $P_R$ , emerges from the  $Q_1$  state.

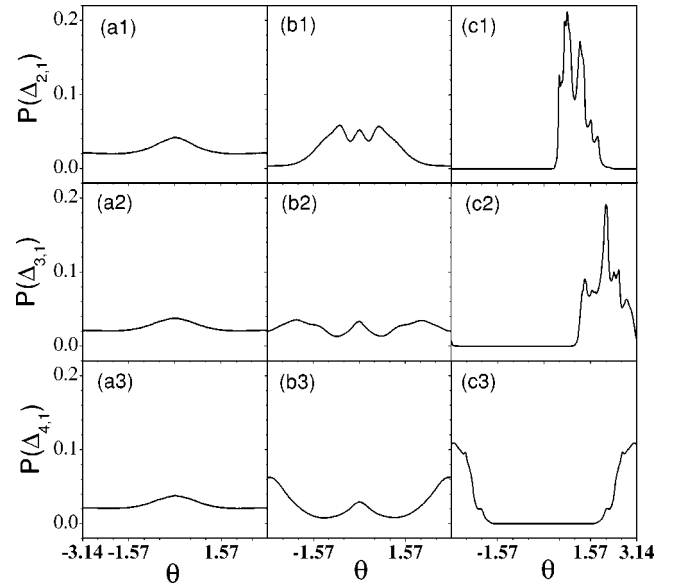


FIG. 3. Probability distributions of angle differences  $\Delta_{2,1}$ ,  $\Delta_{3,1}$ , and  $\Delta_{4,1}$  for different  $\varepsilon$ . (a1)–(a3)  $\varepsilon=0.002$ . (b1)–(b3)  $\varepsilon=0.012$ . (c1)–(c3)  $\varepsilon=0.020$ .

In Fig. 2(e) we show the three largest Lyapunov exponents (LEs) for a global view of the transitions while varying the coupling, in which all the states mentioned above are marked. In this figure the transitions between  $C_A$ ,  $P_6$ ,  $P_2$ ,  $Q_1$ , and  $P_R$  are clearly identified by the characteristic changes of the LE’s. Actually, the transition from  $C_A$  to  $P_6$  is through the inverse period-doubling bifurcations, and that from  $Q_1$  to  $P_R$  is through an inverse Hopf bifurcation. The bifurcations between  $P_6$ ,  $P_2$ , and  $Q_1$  are slightly complicated. We will not go into the detail of these bifurcations since they all link various regular states. The most interesting transition in Fig. 2 is the one between  $C_D$  and  $C_A$ . This transition, occurring between two high-dimensional chaotic states, is not identified in Fig. 2(e) by any discontinuity of the first three largest Lyapunov exponents, in sharp contrast with all other transitions previously mentioned. Now let us study this transition in more detail.

We define the phase difference between any given sites by comparing them with a reference site, which is arbitrarily chosen as the first one  $\Delta_{i,1}(t) = \arctan[y_i(t)/x_i(t)] - \arctan[y_1(t)/x_1(t)]$ .  $\Delta_{i,1}(t)$  must fluctuate in both  $C_D$  and  $C_A$  states due to their chaoticity. However, their statistical behaviors should respond to the transition from  $C_D$  to  $C_A$ . The time step for computation is 0.01, and the steps for our Rössler oscillators to rotate  $2\pi$  in the  $(x,y)$  plane, i.e., to make a cycle, is about 628. We compute the probability distribution of  $\Delta_{i,1}$  by a sample of time steps as  $10^7$  starting from having cutoff a  $10^6$  transient. Figure 3 shows the distributions of  $\Delta_{i,1}$ ,  $i=2,3$ , and 4 for three different coupling intensities. With a very small coupling [(a1)–(a3),  $\varepsilon=0.002$ ] all  $n$  oscillators are nearly uncorrelated from each other, and then the distributions are similar to that of an individual oscillator, which is peaked at zero angle, and the influence of the coupling is practically not felt. Increasing  $\varepsilon$  to a certain extent, the structure of the distribution undergoes

a characteristic change seen in (b1)–(b3) ( $\varepsilon=0.012$ ), and the distributions of  $\Delta_{i,1}$  form some additional peaks away from the zero angle and they are centered at  $\Delta_{i,1} \approx \pm 2\pi(i-1)/6$ . These localized distributions represent a primary step for the phase ordering. However, in (b) no orientational priority exists. In Figs. 3(b1)–3(b3) the probabilities are distributed symmetrically in both positive and negative directions. When  $\varepsilon$  is increased further, the balance between the two side peaks break, and  $\Delta_{2,1}$  and  $\Delta_{3,1}$  have a choice to locate their distribution peaks on only one side, either the positive or negative side, depending on the initial condition [see Figs. 3(c1)–3(c3),  $\varepsilon=0.020$ ]. Thus a spontaneous phase ordering, associated to the orientational equality breaking occurs, which is the key element for the spatial order of the rotating wave. The changing from Fig. 3(a) to 3(c) is a typical phase synchronization between chaotic oscillators [10]; a significant new feature in our case is that this phase synchronization of the chaotic element leads to a phase locking with an equal phase separation distribution in the long-time average, the so-called average-antiphase distribution. The crossover region can be narrower if we increase the number of coupled oscillators  $n$ , in our simulation. It is very probable that a (sharp) transition may be observed in the large  $n$  limit (so-called thermodynamic limit) [11]. However, for large  $n$ , different antiphase states with various  $k$  (where  $k$  is the period of the mode of antiphase state we will discuss later) can coexist, which makes a convincing judgement of (sharp) transition difficult. This difficulty will be treated in a future work; here the word “transition” is loosely used to describe this crossover. The rotating wave can be approached step-by-step as  $\varepsilon$  increases, and the temporal behavior changes from chaos to periodicity improving the spatial order shown in Fig. 3(c).

The above transition route is independent of the specific coupling configurations. In this paper we applied the couplings for all the three coordinates  $(x,y,z)$ , which can be written as a (111) configuration. We have checked systems with a number of other coupling forms such as (100), (010), (110), (011), and (101); in all these cases we observe the typical rotating wave developed from spatiotemporal chaos, following the same transition route as in Figs. 2 and 3. Moreover, the transition route is also independent of the number of cells. We have confirmed its generality by computing Eqs. (1) for different  $n$ , like  $n=5, 7, 14, 15, 50, 200$ , and 500, and find the similar results in all cases tested. Other interesting observations are (i) chaos with average-antiphase and the resulting rotating waves cannot appear for small systems  $n < 5$ , and (ii) for large  $n$  the system can develop rotating waves with larger wave numbers  $k > 1$ , i.e., the phase shift between neighboring cells is  $2k\pi/n$ ,  $k > 1$ , rather than  $2\pi/n$ . In Fig. 4 we do the same as Figs. 1 and 2 by taking  $n=14$ . The results show a spatially disordered chaos in Fig. 4(a) for small coupling  $\varepsilon=0.015$ , a chaotic state with  $k=2$  ordered average-antiphase distribution in Fig. 4(b) for slightly larger coupling  $\varepsilon=0.0187$ , and a  $k=2$  periodic rotating wave [the neighbor phase shift is  $\Delta_{i+1,i}=4\pi/n$  in Fig. 4(c) for  $\varepsilon=0.069$ ]; and another  $k=1$  rotating wave with neighbor phase shift  $\Delta_{i+1,i}=2\pi/n$  by further increasing the coupling to  $\varepsilon=0.340$ .

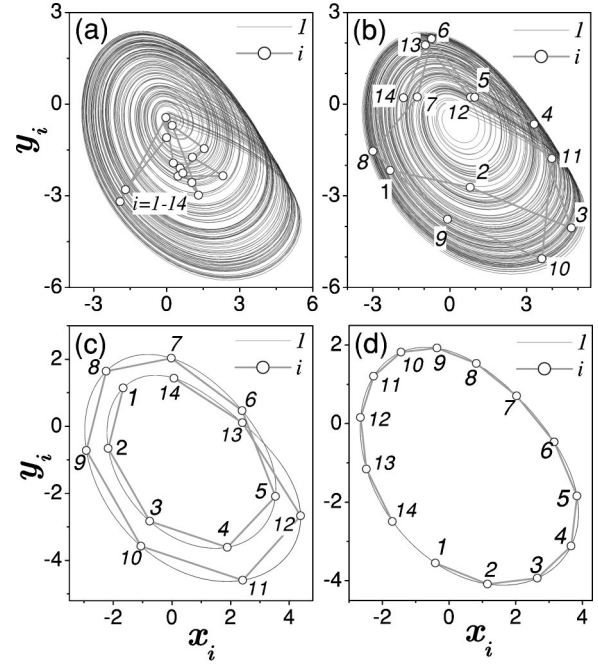


FIG. 4. Orbits of the system with  $n=14$ . (a)  $\varepsilon=0.015$ , chaos with spatially disordered phase distribution. (b)  $\varepsilon=0.0187$ , chaotic and average-antiphase state with  $k=2$ . (c)  $\varepsilon=0.069$ , periodic rotating wave of  $k=2$ . (d)  $\varepsilon=0.340$ , periodic rotating wave of  $k=1$ .

A significant point is that all the above observations can be intuitively understood, based on the competition of two facts, chaos and coupling. For small coupling, chaos succeeds in making the spatial distribution disordered, while the mutual coupling is in favor to drive the oscillators to certain spatial orders characterized by the minima of the coupling “potential.” Focusing on the chaotic motion in  $(x,y)$  space and neglecting the amplitude fluctuation of the oscillators, i.e., setting the motion as  $x_i(t)=r \cos \phi_i(t)$ ,  $y_i(t)=r \sin \phi_i(t)$ , we can describe the couplings of Eqs. (1) in the  $(x,y)$  plane as a gradient force of a potential

$$\begin{aligned}
 H(\vec{\phi}) &= \sum_{i=1}^n \frac{1}{2} r^2 \{ [\sin(\phi_{i+1}) - \sin(\phi_i)]^2 \\
 &\quad + [\cos(\phi_{i+1}) - \cos(\phi_i)]^2 \} \\
 &= r^2 \left[ n - \sum_{i=1}^n \cos(\Delta_{i+1,i}) \right],
 \end{aligned}$$

$$\vec{\phi} = (\phi_1, \phi_2, \dots, \phi_n) \quad (3)$$

and the coupling intends to bring the phase distribution to the minima of this potential. It is easy to show that at the distributions with equal phase separations

$$\Delta_{2,1} = \Delta_{3,2} = \dots = \Delta_{1,n} = \Delta = \frac{2k\pi}{n}, \quad k=1, 2, \dots, \leq \frac{n}{2} \quad (4)$$

the potential has extrema values  $\partial H(\vec{\phi})/\partial \phi_i = 0$ ,  $i=1, 2, \dots, n$ . The necessary and sufficient condition for any

of these extrema to be minima is  $\cos \Delta > 0$ , i.e.,  $|\Delta| < \pi/4$ . Thus, for an antiphase state  $\Delta = 2k\pi/n$  to have a minimal potential, the system size should be  $n > 4k$ . Now we are able to understand the main results of this paper in terms of the chaos-coupling competition. Let us take the  $k=1$  wave (Figs. 1–3) as our example. For  $n < 4$ , both chaos and coupling do not support the ordered antiphase state. Consequently, no periodic rotating wave is observable. For  $n > 4$ , the coupling can support some ordered configurations of Eq. (4) with minimal potential, however, the chaos still wants to destroy any ordering, their competition leads to different results for different coupling intensities.

For very small coupling ( $\varepsilon < \varepsilon_0$ ), chaos dominates, producing random-phase distribution [Figs. 1(a) and 3(a)]; by increasing  $\varepsilon$ , the coupling can overcome the chaos influence and drive the system to the vicinity of an antiphase state of Eq. (4) from time to time. This leads to the distributions of Fig. 3(b), peaked at the positions of the phase shifts of one of the minimum states of Eq. (4). However, in Fig. 3(b) chaos is still strong enough to push the system away from the ordered state. So, the system switches from random spatial order to the phase ordering, either clockwise or anticlockwise, and generates the localized while symmetric probability distributions of Fig. 3(b). By further increasing  $\varepsilon$ , the coupling starts to dominate and the oscillators have to remain in a well of a minimum of the coupling potential. Chaos can produce only small fluctuations of the phase distribution around the antiphase state established, and can no longer destroy it; this leads to the stable phase ordering and orientational equality

breaking in Figs. 1(b) and 3(c), which are the most important elements of the spatial order for the corresponding periodic rotating wave. A similar argument can be applied to the antiphase states with larger wave number  $k > 1$ . It is emphasized that the antiphase states with different  $k$  can coexist when the potential Eq. (4) has multiple minima. We will not go into the detail of the matter of multistability. It is worthwhile remarking that the in-phase state ( $k=0$ ) occupies all possible symmetries a ring geometry can have. Since considerably large coupling is needed to balance all the oscillators into spatial order higher than  $Z_n$ , the in-phase state can appear only for rather large  $\varepsilon$ , though this state has minimal potential for arbitrary system size  $n > 1$ .

In summary, we have investigated a transition route from spatiotemporal chaos to rotating waves. A phase synchronization transition between chaotic oscillators is found to be crucial. This chaos synchronization leads to an orientational symmetry breaking and the associated average-antiphase organization, from which the spatial order of the rotating wave is formed. In studying this problem, ring-coupled Rössler oscillators are taken as our model. Rings of coupled oscillators have long ago been advocated as useful models in many physics, chemistry, and biology contexts. We hope the results in the present paper can be found useful for both theoretical study and experimental investigation in exploring the origins of various ordering in disordered chaotic systems.

This work was partially supported by the National Natural Science Foundation of China and the Nonlinear Science project of China.

- 
- [1] A.M. Turing, *Philos. Trans. R. Soc. London, Ser. B* **237**, 37 (1952).
- [2] G. Szekely, *Acta Phys. Acad. Sci. Hung.* **27**, 285 (1965); F. Delcomyn, *Science* **210**, 492 (1980); H. Cruse, *Trends Neurosci.* **13**, 15 (1990).
- [3] D.F. Hoyt and R.C. Taylor, *Nature (London)* **292**, 239 (1981); S. Grillner and P. Wallen, *Annu. Rev. Neurosci.* **8**, 233 (1985); J.J. Collins and Ian Stewart, *Biol. Cybern.* **68**, 287 (1993), and references therein.
- [4] P. Hadley and M.R. Beasley, *Appl. Phys. Lett.* **50**, 621 (1987); D.G. Aronson, E.J. Doedel, and H.G. Othmer, *Int. J. Bifurcation Chaos Appl. Sci. Eng.* **1**, 51 (1991); S. Watanabe and S.H. Strogatz, *Physica (Amsterdam)* **74D**, 197 (1994).
- [5] R. Van Buskirk and C. Jeffries, *Phys. Rev. A* **31**, 3332 (1985); P. Ashwin, *Nonlinearity* **3**, 603 (1990); J. Guemez and M.A. Matias, *Phys. Rev. E* **52**, R2145 (1995).
- [6] K. Wiesenfeld, C. Bracilowski, G. James, and R. Roy, *Phys. Rev. Lett.* **65**, 1749 (1990); J.L. Rogers and L.T. Wille, *Phys. Rev. E* **54**, R2193 (1996); C. Diorio and R.P.N. Rao, *Nature (London)* **405**, 891 (2000).
- [7] J.F. Heagy, T.L. Carroll, and L.M. Pecora, *Phys. Rev. E* **50**, 1874 (1994); J.F. Heagy, L.M. Recora, and T.L. Carroll, *Phys. Rev. Lett.* **74**, 4185 (1995); and see also references in G. Hu, J. Yang, and W. Liu, *Phys. Rev. E* **58**, 4440 (1998).
- [8] G. Hu, Y. Zhang, H.A. Cerdeira, and S. Chen, *Phys. Rev. Lett.* **85**, 3377 (2000).
- [9] M. Golubitsky and I.N. Stewart, *Arch. Ration. Mech. Anal.* **87**, 107 (1985); M. Golubitsky, I.N. Stewart, and D.G. Schaeffer, *Singularities and Groups in Bifurcation Theory* (Springer-Verlag, New York, 1988).
- [10] M.G. Rosenblum, A.S. Pikovsky, and J. Kurths, *Phys. Rev. Lett.* **76**, 1804 (1996); E. Rosa, E. Ott, and M.H. Hess, *ibid.* **80**, 1642 (1998); Z. Zheng, G. Hu, and B. Hu, *ibid.* **81**, 5318 (1998).
- [11] C.-K. Hu and C.-Y. Lin, *Phys. Rev. Lett.* **77**, 8 (1996).